

Appendix A: Specific heat tests

- ON-Kallo1-103a-mod $e=0.71$ $Sr=0.71$

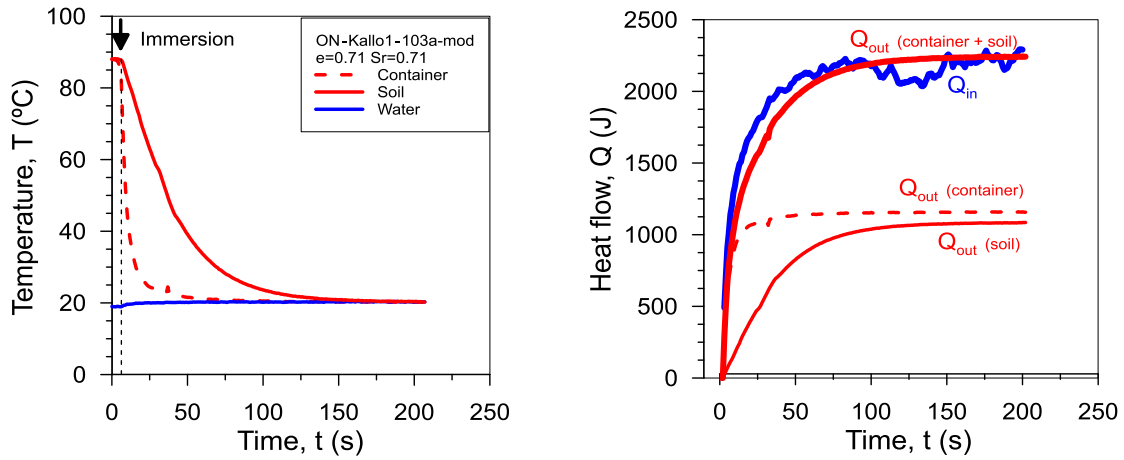


Fig. 1 Specific heat test, (a.) Time evolution of temperature and (b.) Time evolution curve of total Q_{out} to Q_{in} .

- ON-Kallo1-103a-mod $e=0.60$ $Sr=1.00$

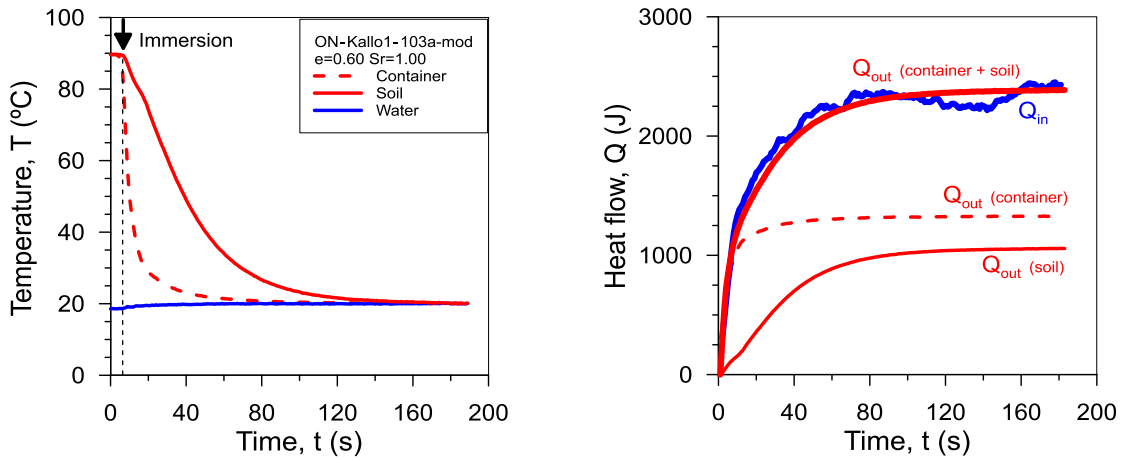


Fig. 2 Specific heat test, (a.) Time evolution of temperature and (b.) Time evolution curve of total Q_{out} to Q_{in} .

- ON-Kallo1-103a-mod $e=0.72$ $Sr=1.00$

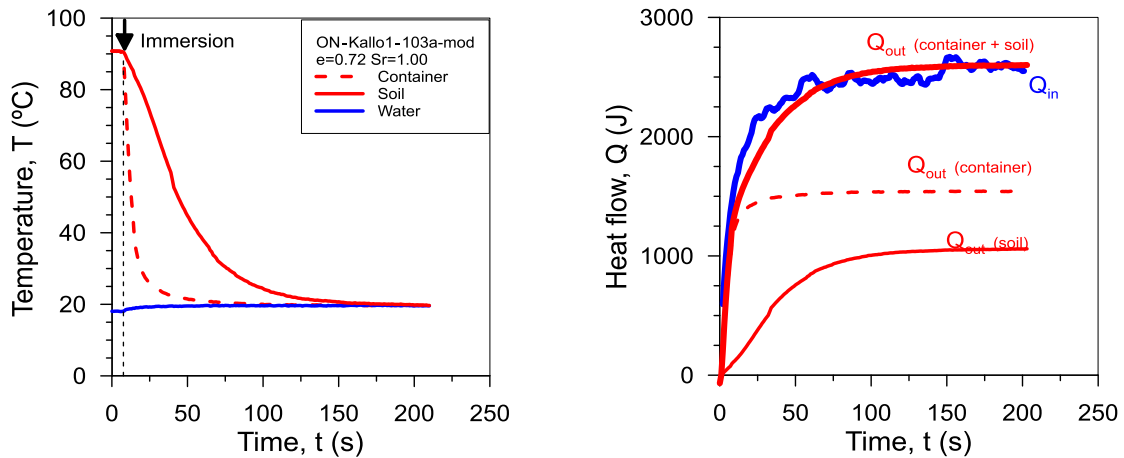


Fig. 3 Specific heat test, (a.) Time evolution of temperature and (b.) Time evolution curve of total Q_{out} to Q_{in} .

Thermal properties in artificially prepared samples mimicking deep Ypresian clays
Appendices

▪ ON-Kallo1-103a-mod $e=0.88$ $Sr=1.00$

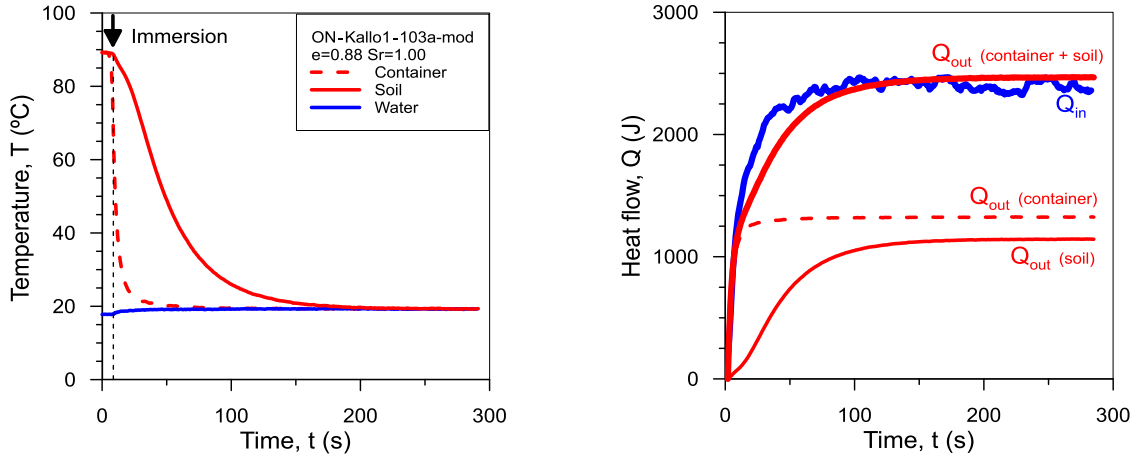


Fig. 4 Specific heat test, (a.) Time evolution of temperature and (b.) Time evolution curve of total Q_{out} to Q_{in} .

▪ ON-Kallo1-022a-mod $e=0.85$ $Sr=1.00$

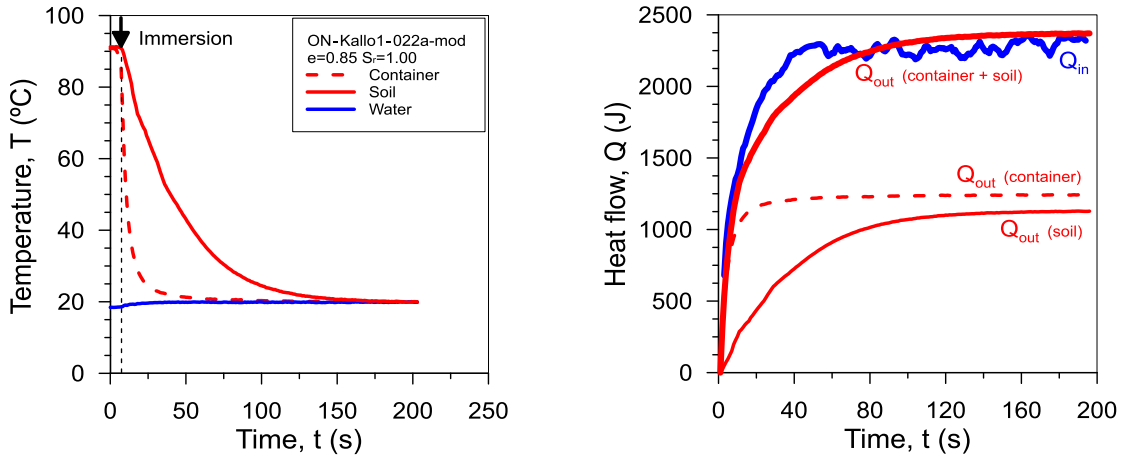


Fig. 5 Specific heat test, (a.) Time evolution of temperature and (b.) Time evolution curve of total Q_{out} to Q_{in} .

▪ ON-Kallo1-022a-mod $e=0.71$ $Sr=0.73$

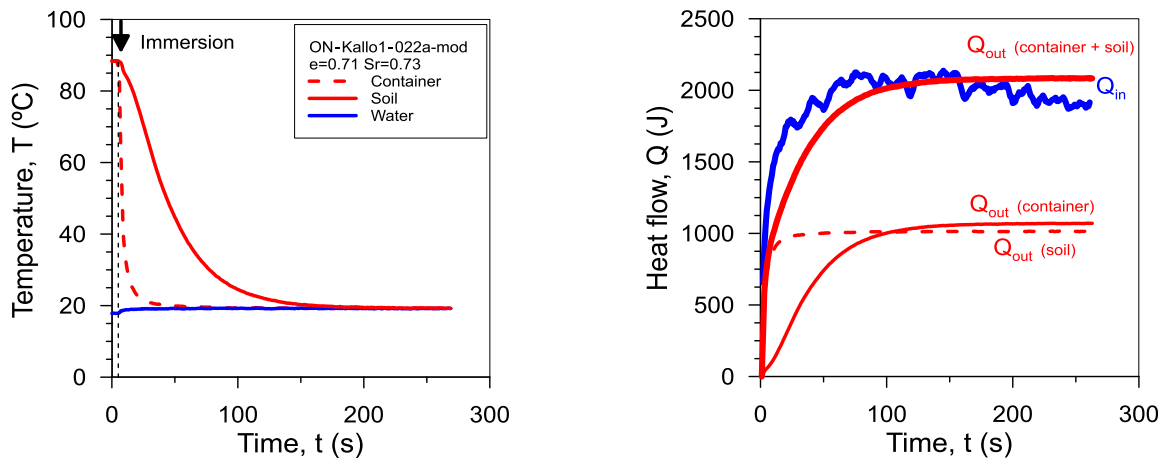


Fig. 6 Specific heat test, (a.) Time evolution of temperature and (b.) Time evolution curve of total Q_{out} to Q_{in} .

Thermal properties in artificially prepared samples mimicking deep Ypresian clays
Appendices

▪ **ON-Kallo1-022a-mod e=0.71 Sr=0.88**

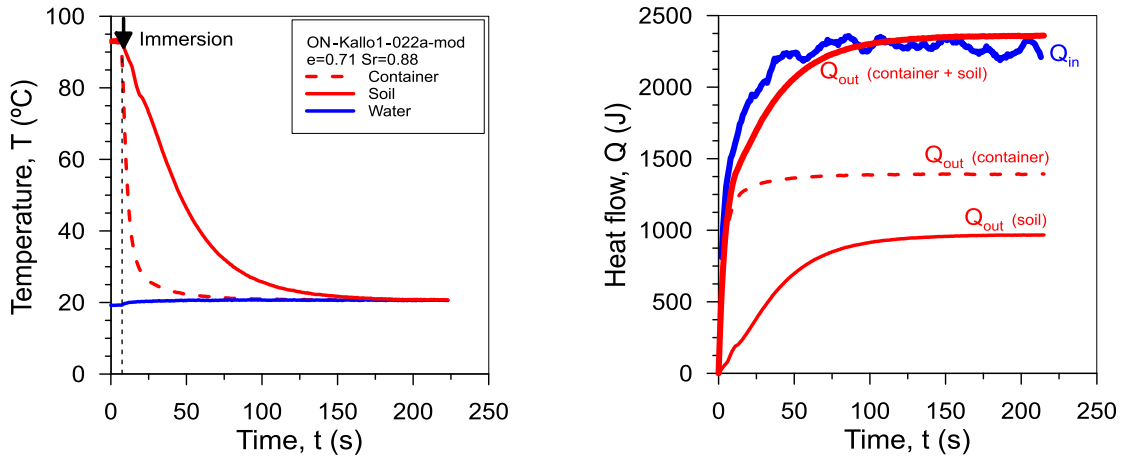


Fig. 7 Specific heat test, (a.) Time evolution of temperature and (b.) Time evolution curve of total Q_{out} to Q_{in} .

▪ **ON-Kallo1-022a-mod e=0.71 Sr=1.00**

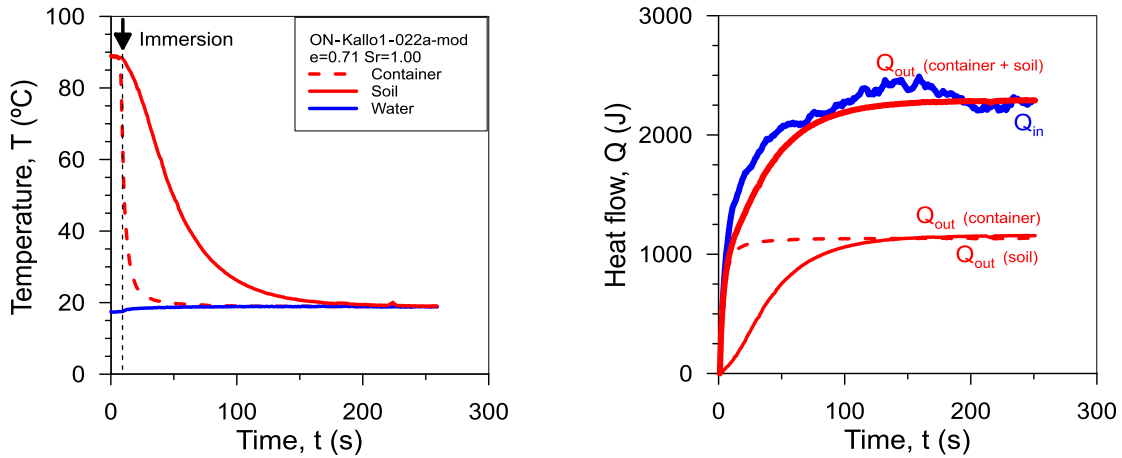


Fig. 8 Specific heat test, (a.) Time evolution of temperature and (b.) Time evolution curve of total Q_{out} to Q_{in} .

▪ **Mix-ON-Kallo1-022a-mod-Qz10% e=0.75 Sr=0.99**

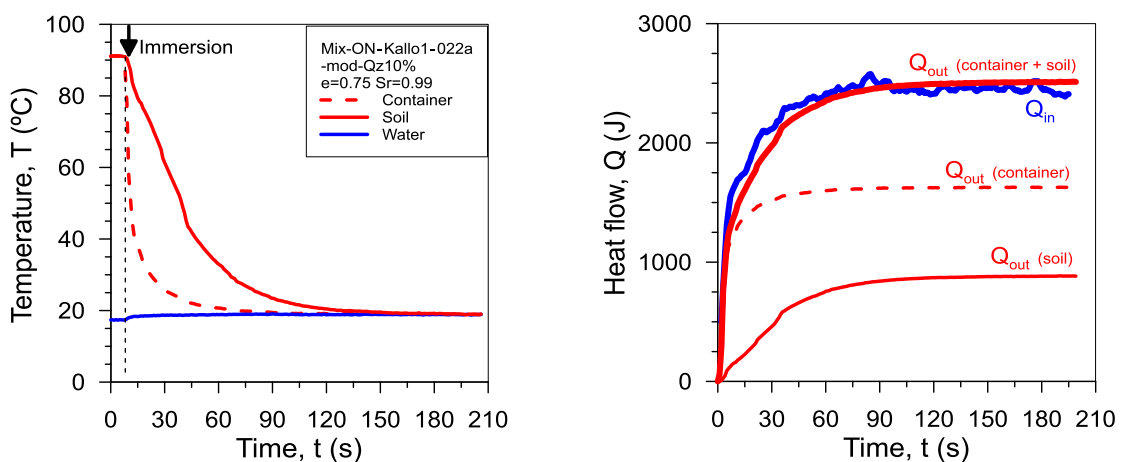


Fig. 9 Specific heat test, (a.) Time evolution of temperature and (b.) Time evolution curve of total Q_{out} to Q_{in} .

Thermal properties in artificially prepared samples mimicking deep Ypresian clays
Appendices

▪ **Mix-ON-Kallo1-022a-Qz-20% $e=0.73$ $Sr=1.00$**

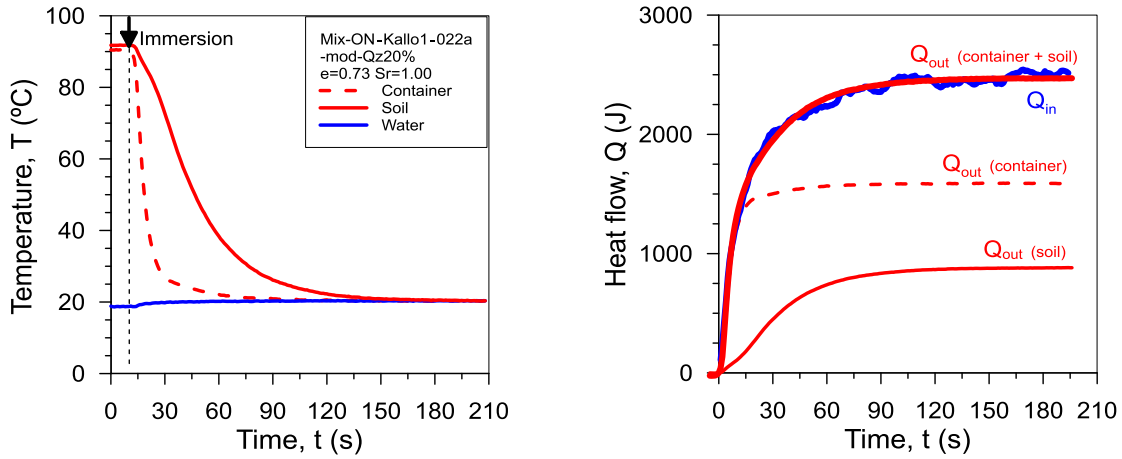


Fig. 10 Specific heat test, (a.) Time evolution of temperature and (b.) Time evolution curve of total Q_{out} to Q_{in}

▪ **Kaolinite $e=0.72$ $Sr=0.93$**

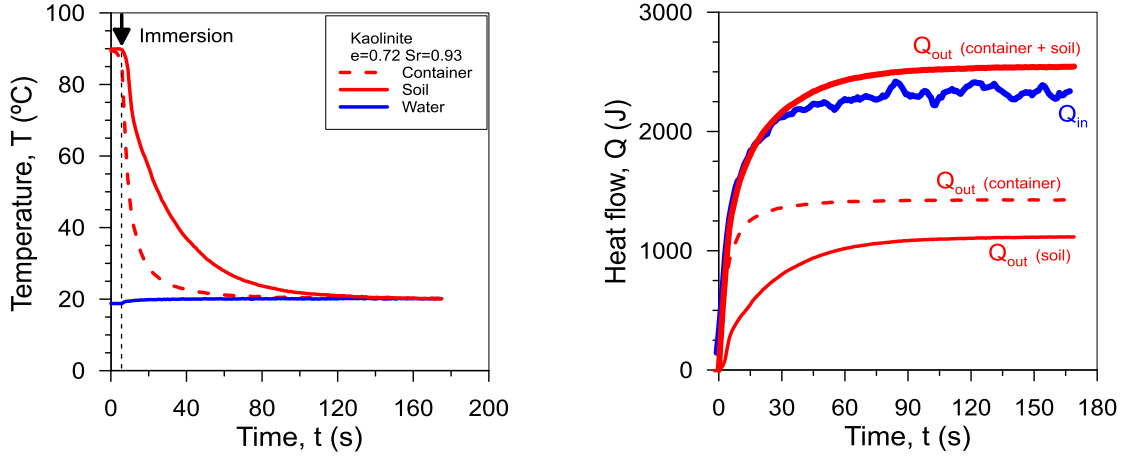


Fig. 11 Specific heat test, (a.) Time evolution of temperature and (b.) Time evolution curve of total Q_{out} to Q_{in} .

▪ **Kaolinite $e=0.80$ $Sr=0.95$**

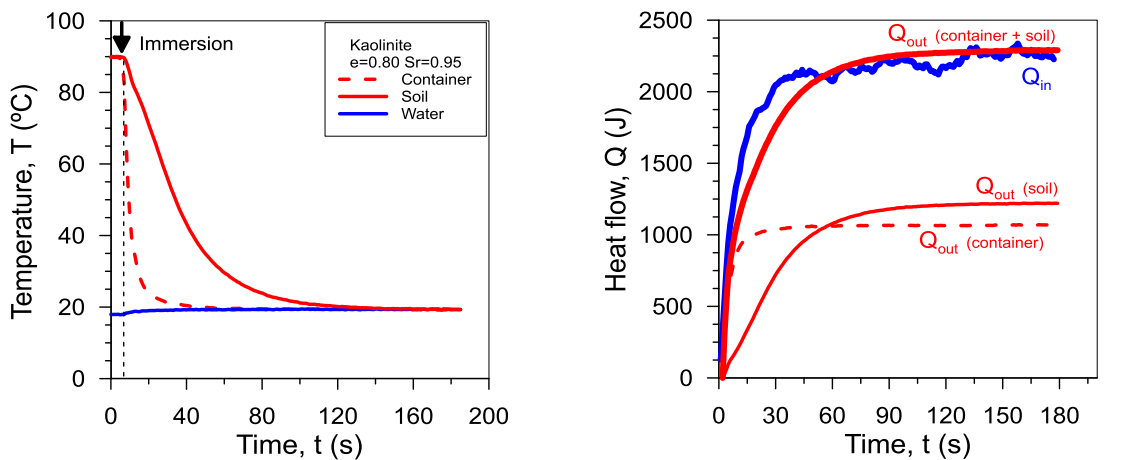


Fig.12 Specific heat test, (a.) Time evolution of temperature and (b.) Time evolution curve of total Q_{out} to Q_{in} .

Thermal properties in artificially prepared samples mimicking deep Ypresian clays
Appendices

▪ Illite $e=0.61$ $Sr=0.98$

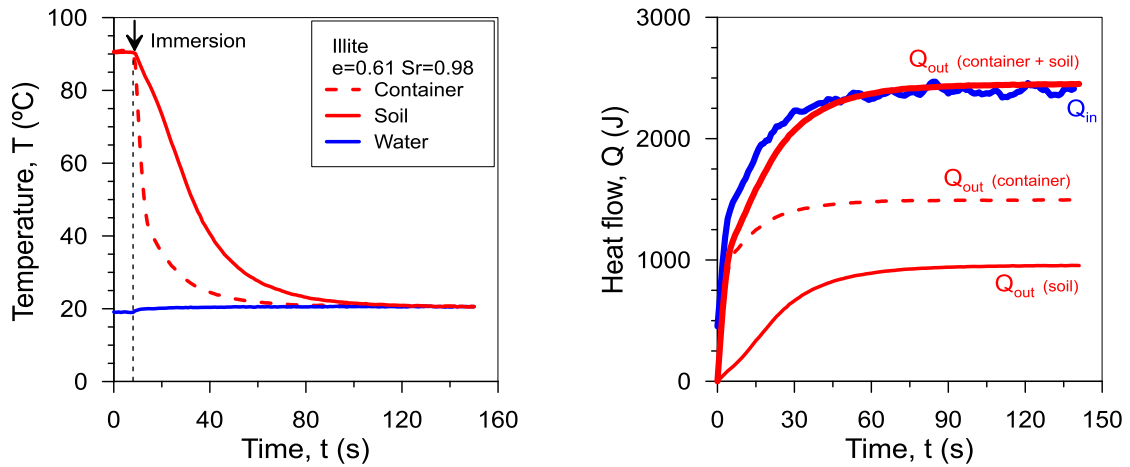


Fig. 13 Specific heat test, (a.) Time evolution of temperature and (b.) Time evolution curve of total Q_{out} to Q_{in} .

▪ Illite $e=0.75$ $Sr=0.83$

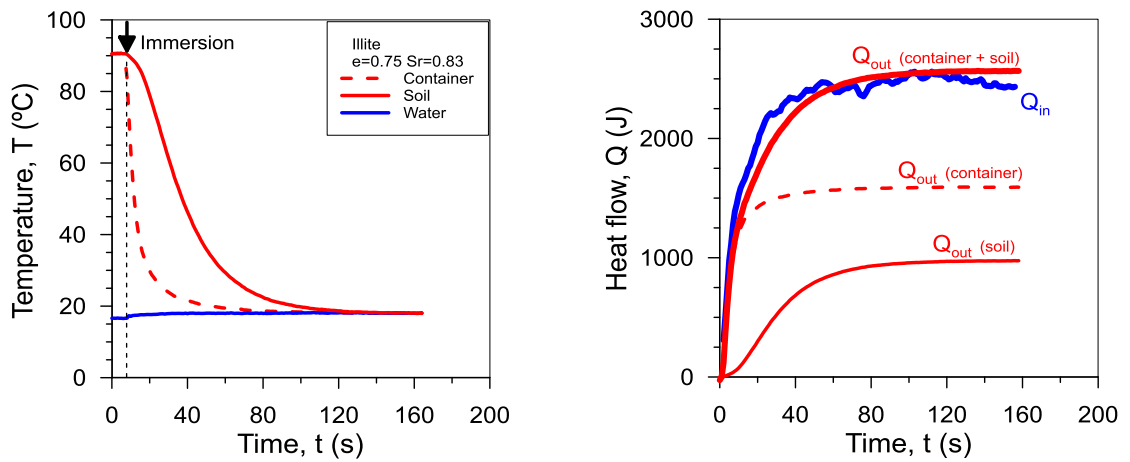


Fig. 14 Specific heat test, (a.) Time evolution of temperature and (b.) Time evolution curve of total Q_{out} to Q_{in} .

Appendix B: Thermal conductivity test

- ON-Kallo1-103a-mod e=0.72 Sr=1.00

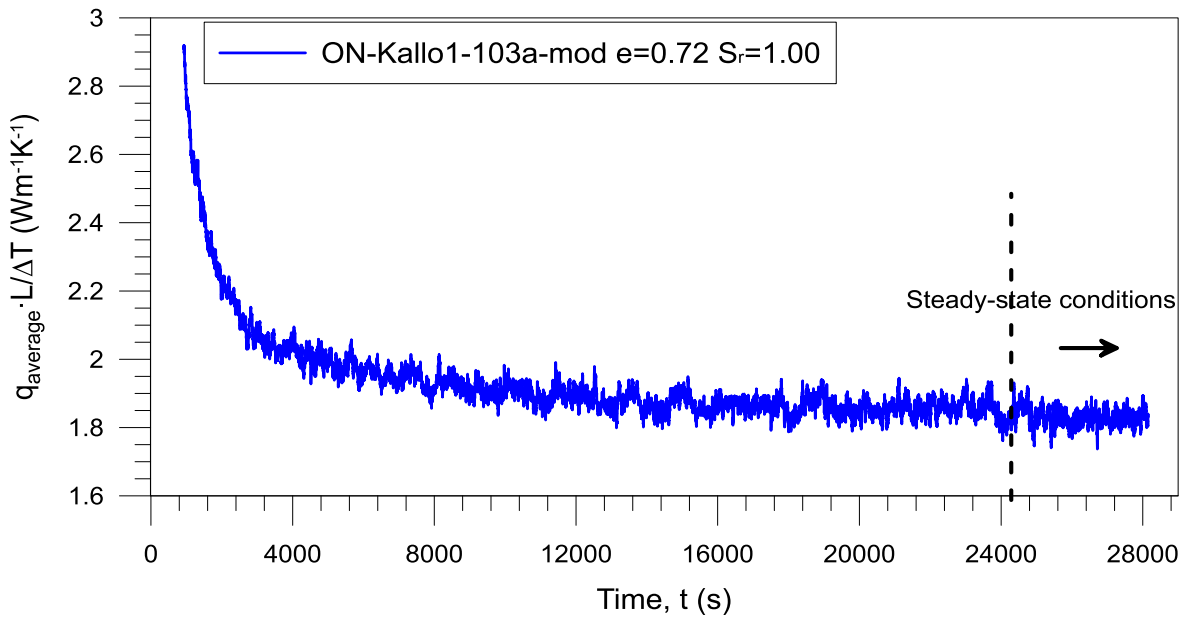


Fig. 15 Time evolution of $q_{\text{ave}} \cdot L / \Delta T$. Thermal conductivity at steady-state conditions for all tests.

- ON-Kallo1-103a-mod e=0.70 Sr=0.70

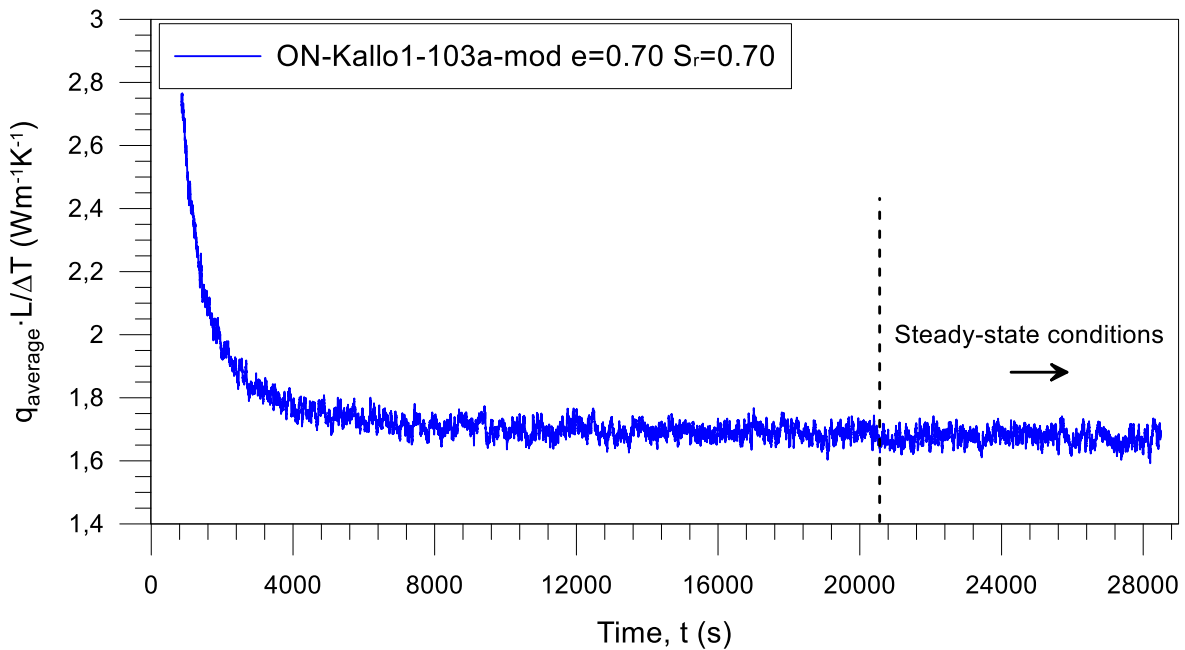


Fig. 16 Time evolution of $q_{\text{ave}} \cdot L / \Delta T$. Thermal conductivity at steady-state conditions for all tests

- ON-Kallo1-103a-mod e=0.69 Sr=0.86

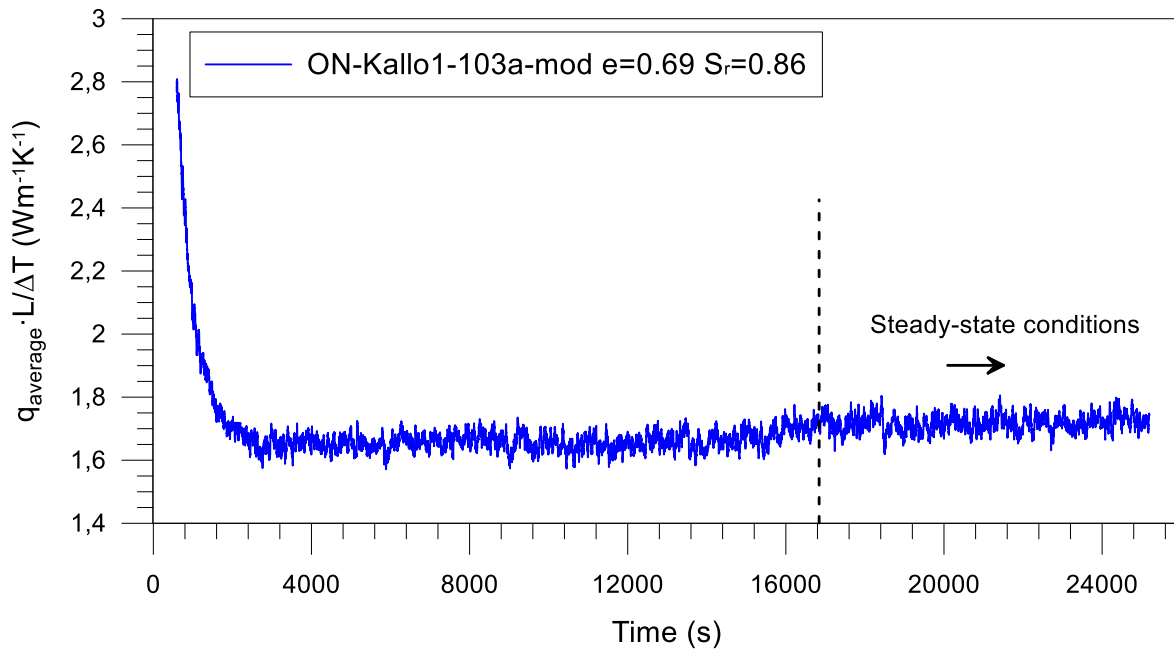


Fig. 17. Time evolution of $q_{ave} \cdot L / \Delta T$. Thermal conductivity at steady-state conditions for all tests.

- ON-Kallo1-103a-mod e=0.59 Sr=1.00

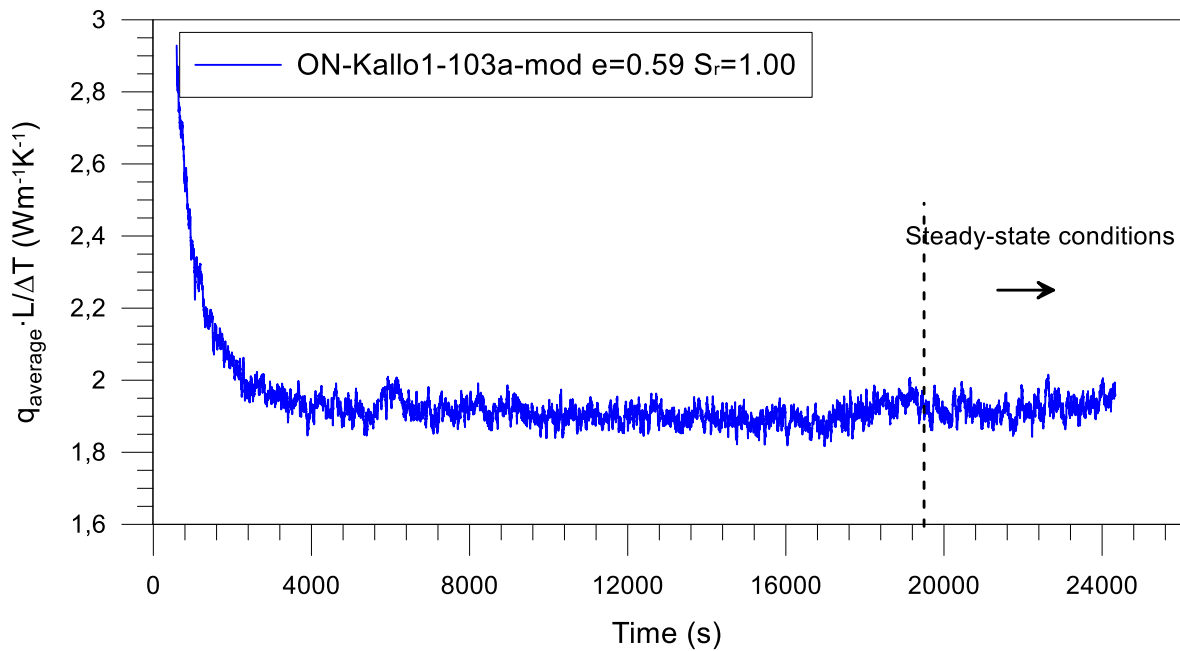


Fig. 18 Time evolution of $q_{ave} \cdot L / \Delta T$. Thermal conductivity at steady-state conditions for all tests

- ON-Kallo1-103a-mod e=0.86 Sr=1.00

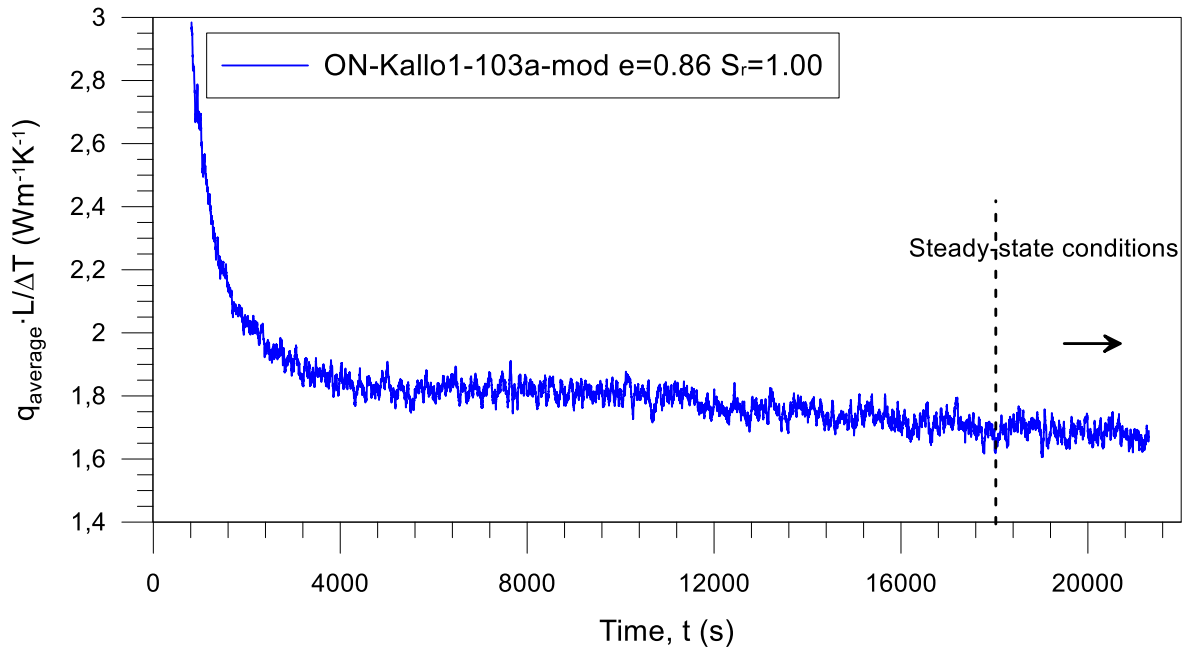


Fig. 19 Time evolution of $q_{ave} \cdot L / \Delta T$. Thermal conductivity at steady-state conditions for all tests.

- ON-Kallo1-022a-mod e=0.71 Sr=1.00

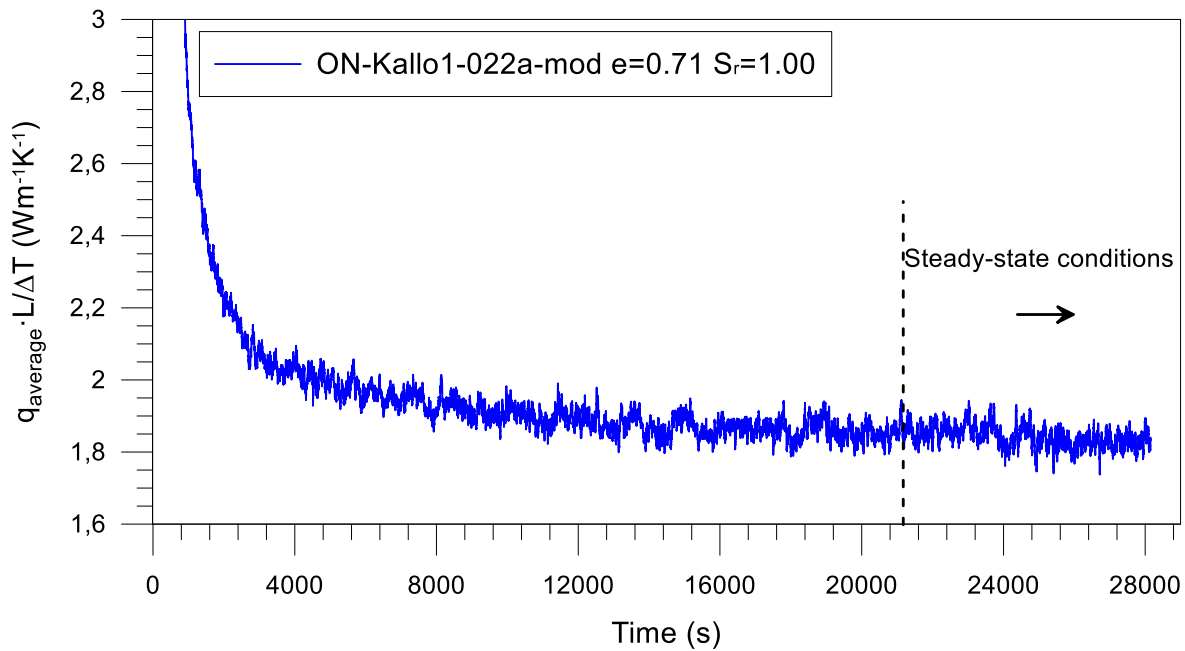


Fig. 20 Time evolution of $q_{ave} \cdot L / \Delta T$. Thermal conductivity at steady-state conditions for all tests.

- ON-Kallo1-022a-mod e=0.68 Sr=0.75

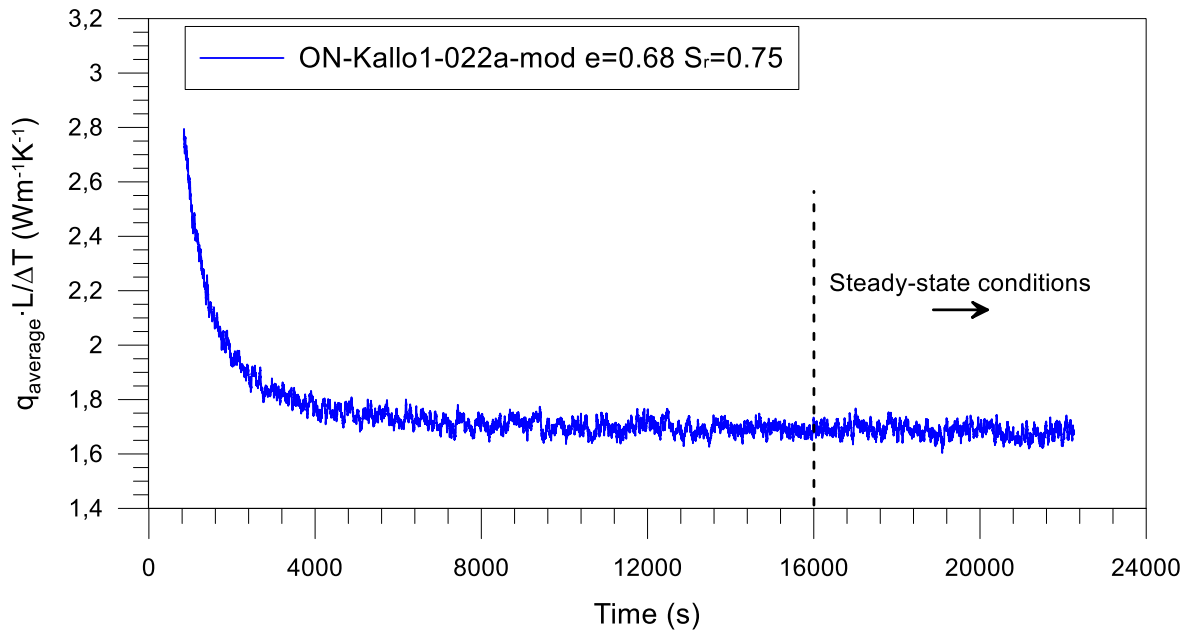


Fig. 21 Time evolution of $q_{\text{ave}} \cdot L / \Delta T$. Thermal conductivity at steady-state conditions for all tests.

- ON-Kallo1-022a-mod e=0.85 Sr=1.00

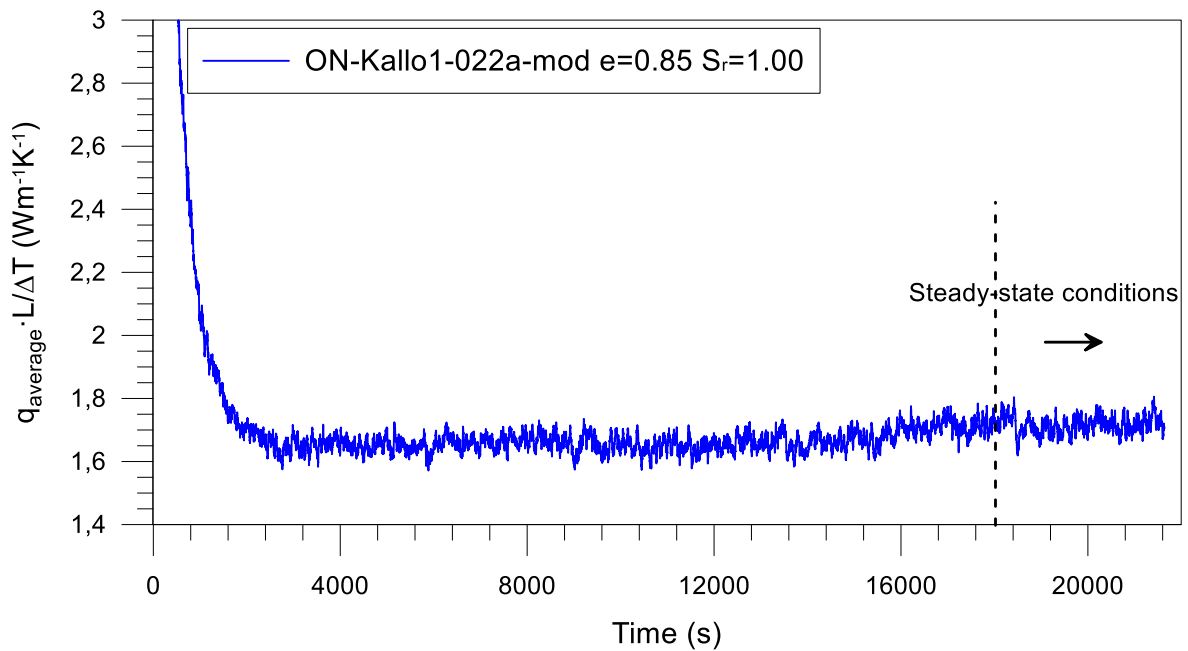


Fig. 22 Time evolution of $q_{\text{ave}} \cdot L / \Delta T$. Thermal conductivity at steady-state conditions for all tests.

- ON-Kallo1-022a-mod e=0.55 Sr=1.00

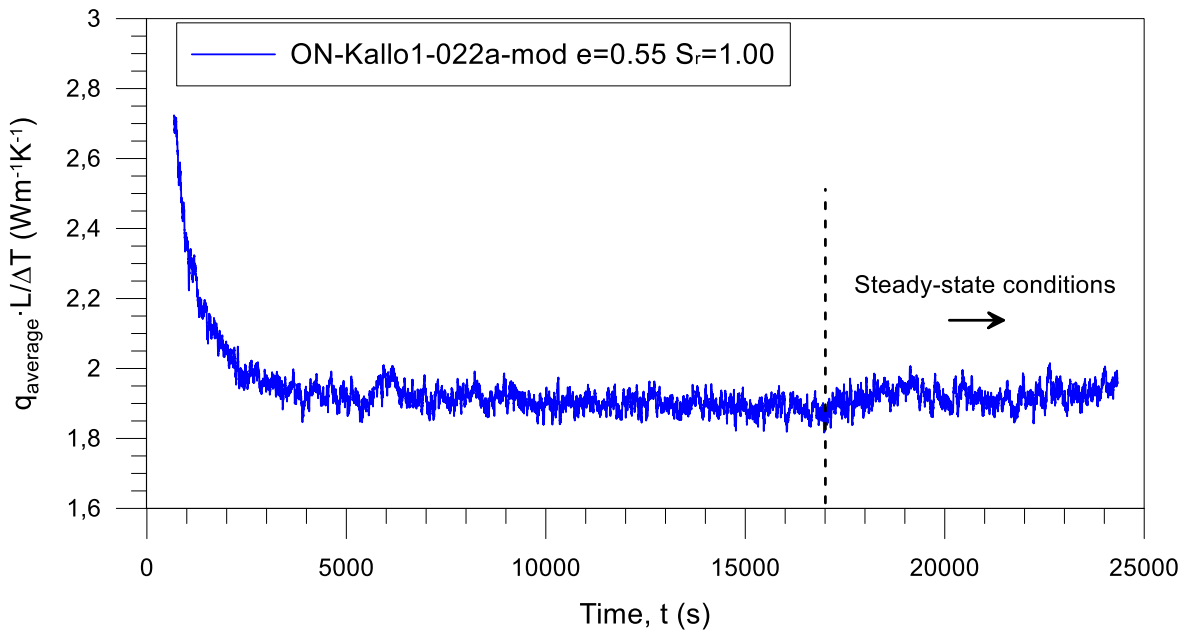


Fig. 23 Time evolution of $q_{ave} \cdot L / \Delta T$. Thermal conductivity at steady-state conditions for all tests.

- ON-Kallo1-022a-mod e=0.70 Sr=0.89

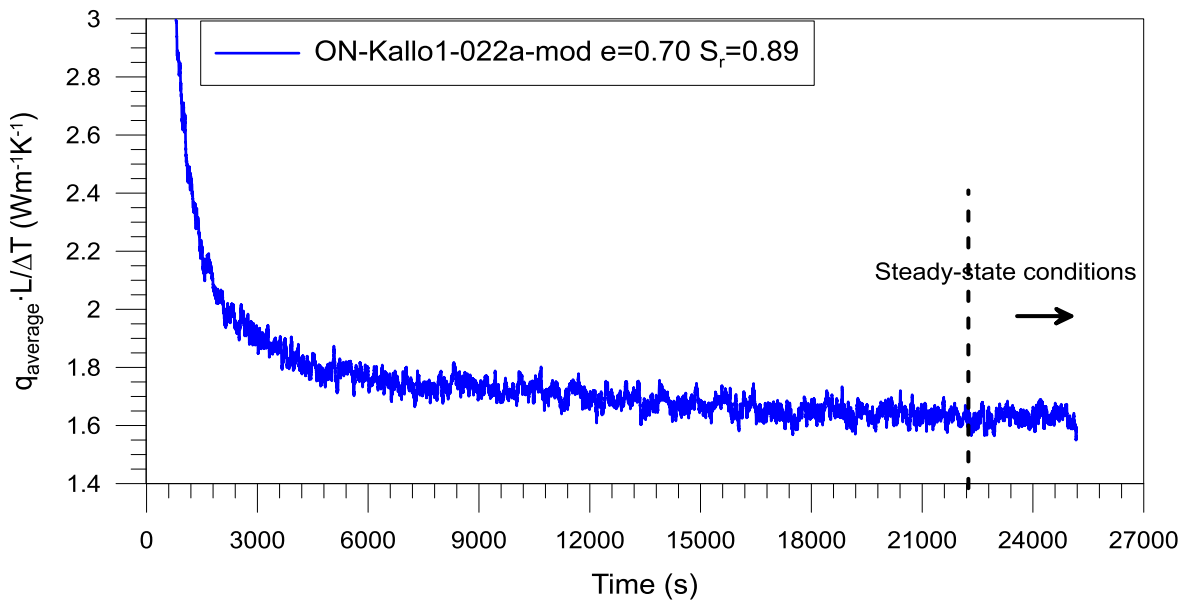


Fig. 24 Time evolution of $q_{ave} \cdot L / \Delta T$. Thermal conductivity at steady-state conditions for all tests.

- Mix-ON-Kallo1-022a-mod-Qz21% e=0.74 Sr=0.98

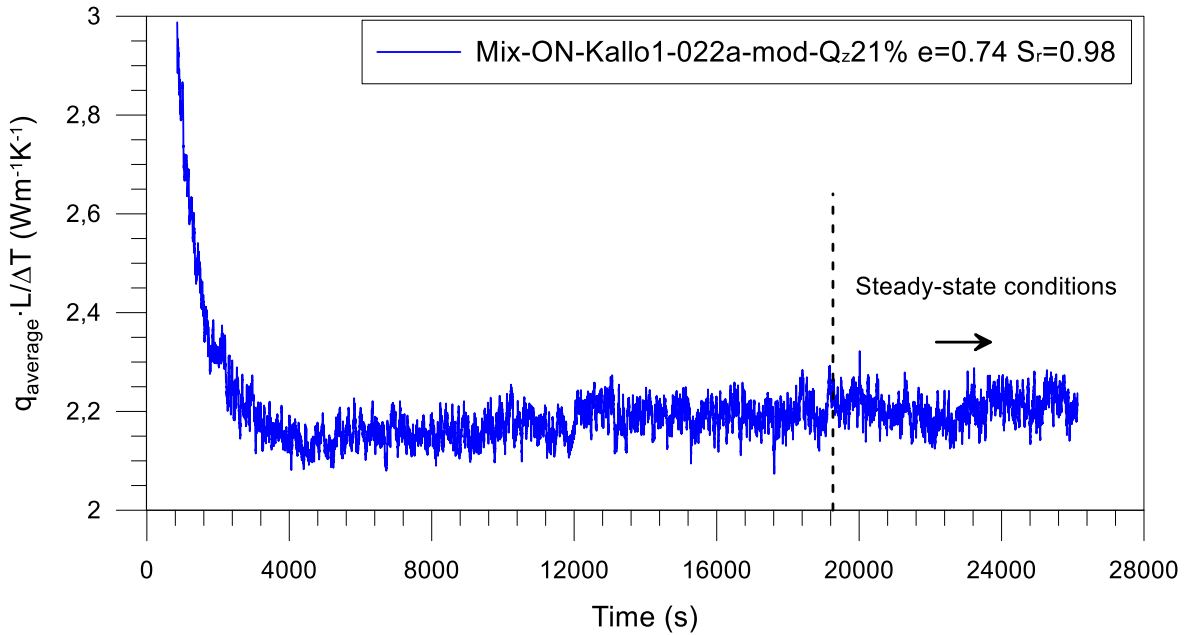


Fig. 25 Time evolution of $q_{ave} \cdot L / \Delta T$. Thermal conductivity at steady-state conditions for all tests.

- Mix-ON-Kallo1-022a-mod-Qz31% e=0.71 Sr=0.85

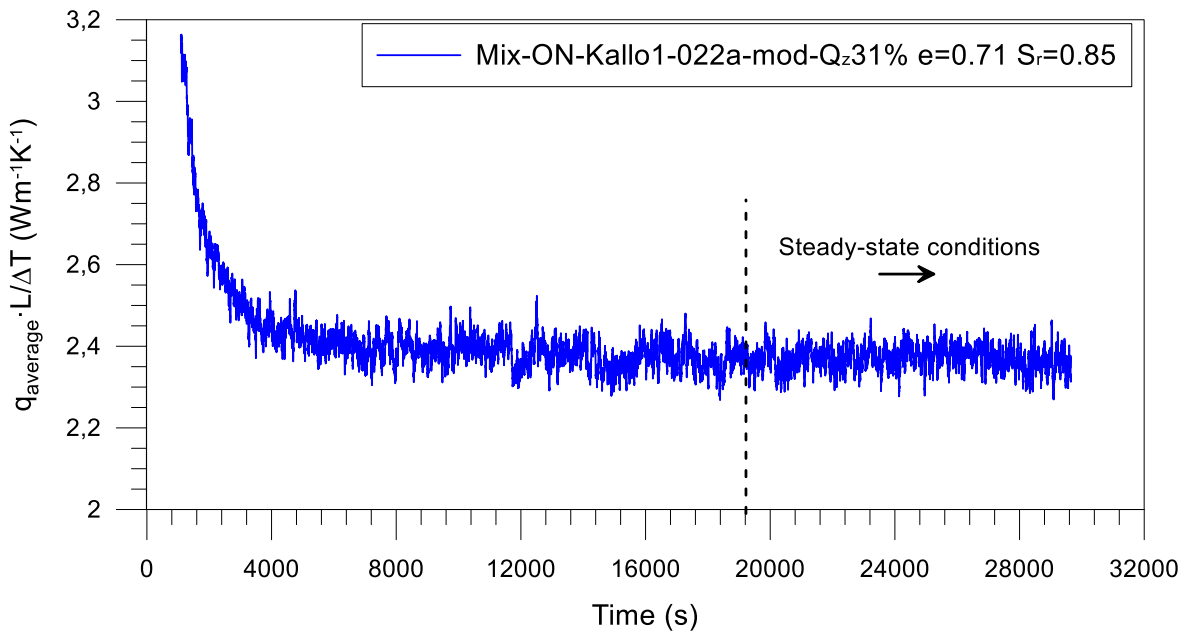


Fig. 26 Time evolution of $q_{ave} \cdot L / \Delta T$. Thermal conductivity at steady-state conditions for all tests.

- Mix-ON-Kallo1-022a-mod-Qz21% e=0.72 Sr=0.69

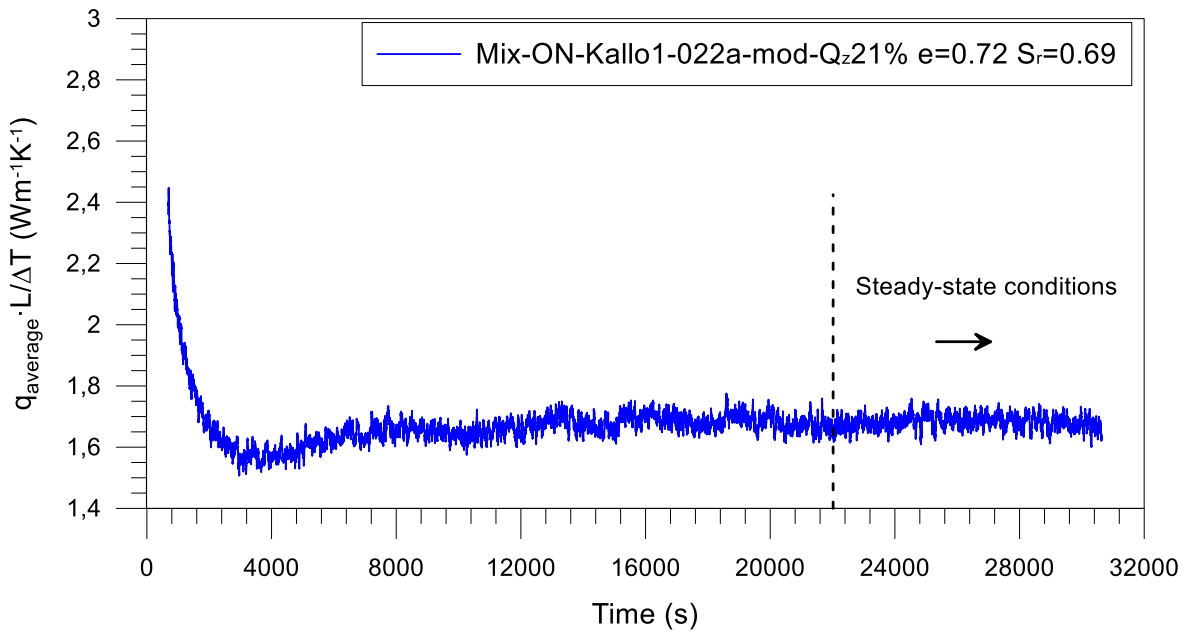


Fig. 27 Time evolution of $q_{ave} \cdot L / \Delta T$. Thermal conductivity at steady-state conditions for all tests.

- Mix-ON-Kallo1-022a-mod-Qz21% e=0.71 Sr=0.84

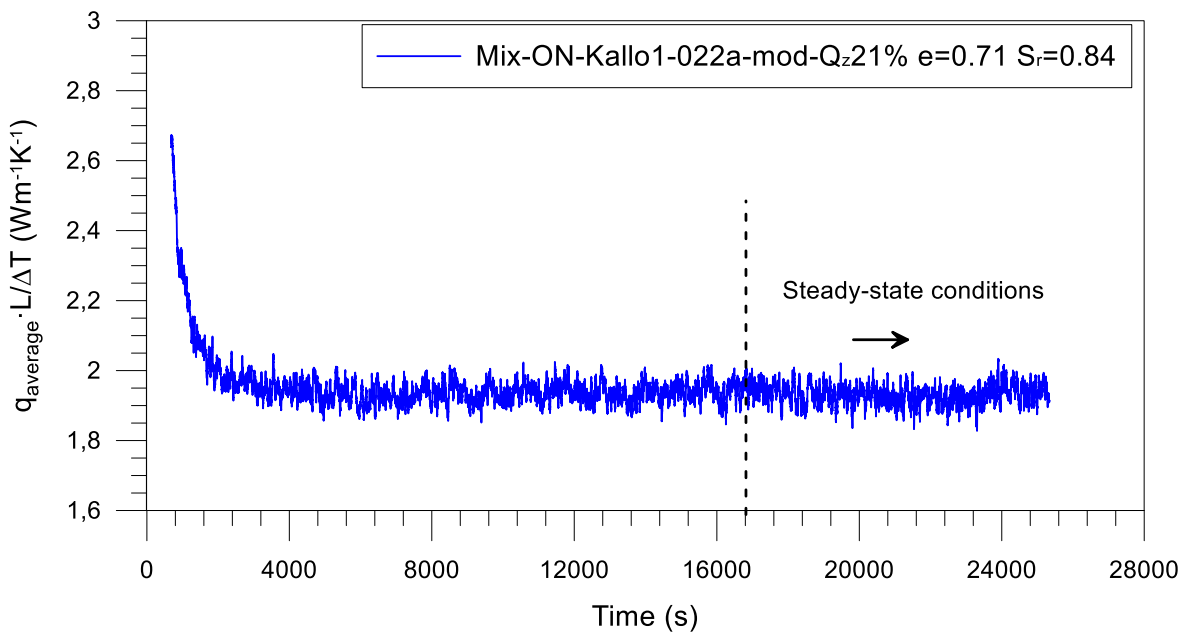


Fig. 28 Time evolution of $q_{ave} \cdot L / \Delta T$. Thermal conductivity at steady-state conditions for all tests.

- Mix-ON-Kallo1-022a-mod-Qz31% e=0.75 Sr=1.00

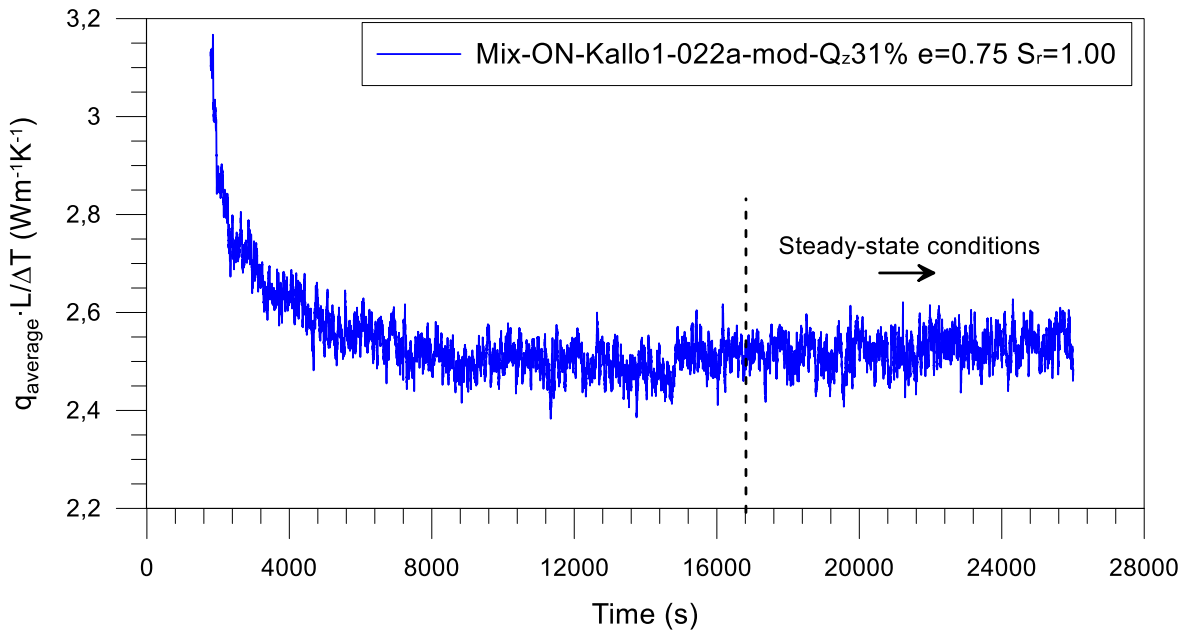


Fig. 29 Time evolution of $q_{ave} \cdot L / \Delta T$. Thermal conductivity at steady-state conditions for all tests.

- Mix-ON-Kallo1-022a-mod-Qz31% e=0.73 Sr=0.71

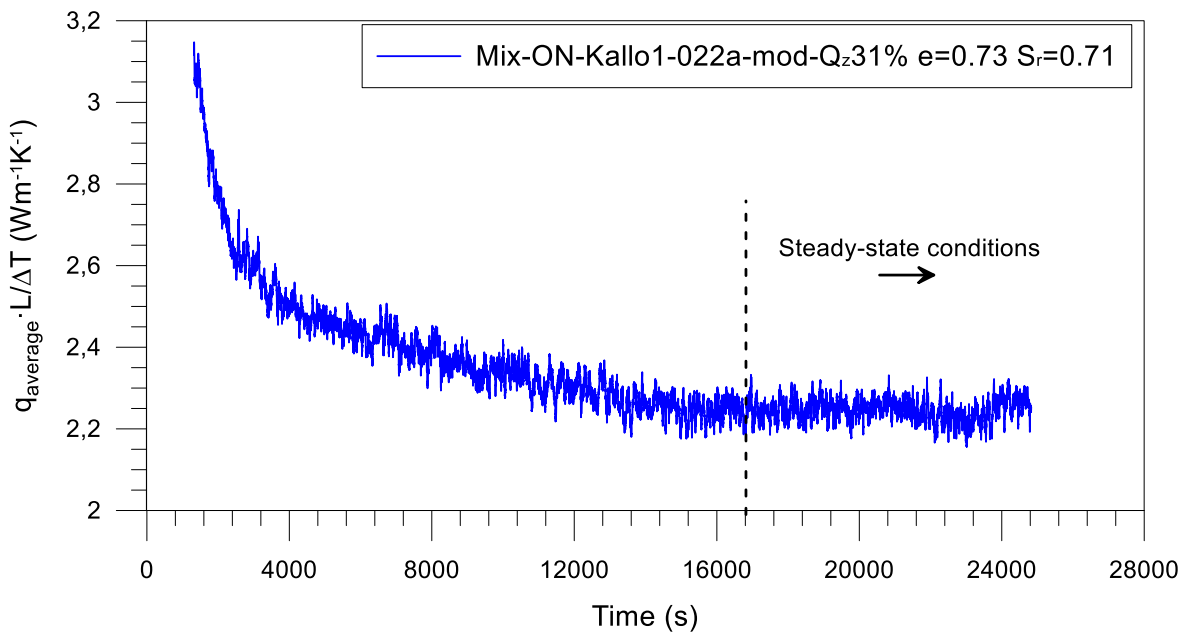


Fig. 30 Time evolution of $q_{ave} \cdot L / \Delta T$. Thermal conductivity at steady-state conditions for all tests.

- Kaolinite e=0.81 Sr=0.80

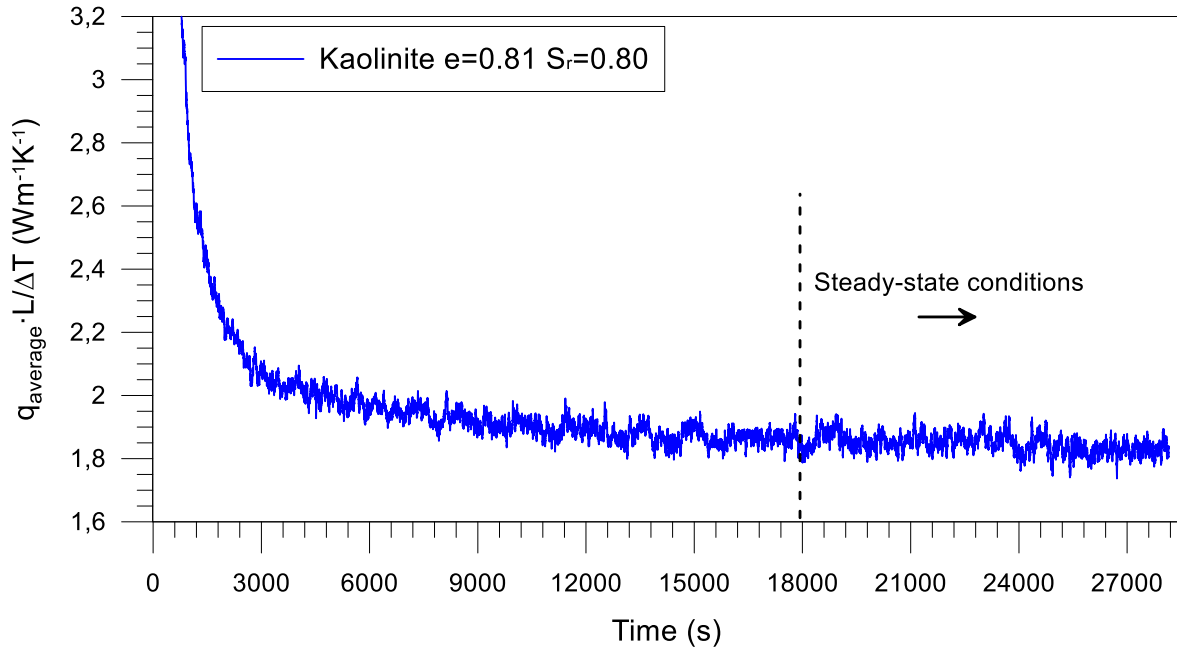


Fig. 31 Time evolution of $q_{ave} \cdot L / \Delta T$. Thermal conductivity at steady-state conditions for all tests.

- Kaolinite e=0.65 Sr=0.83

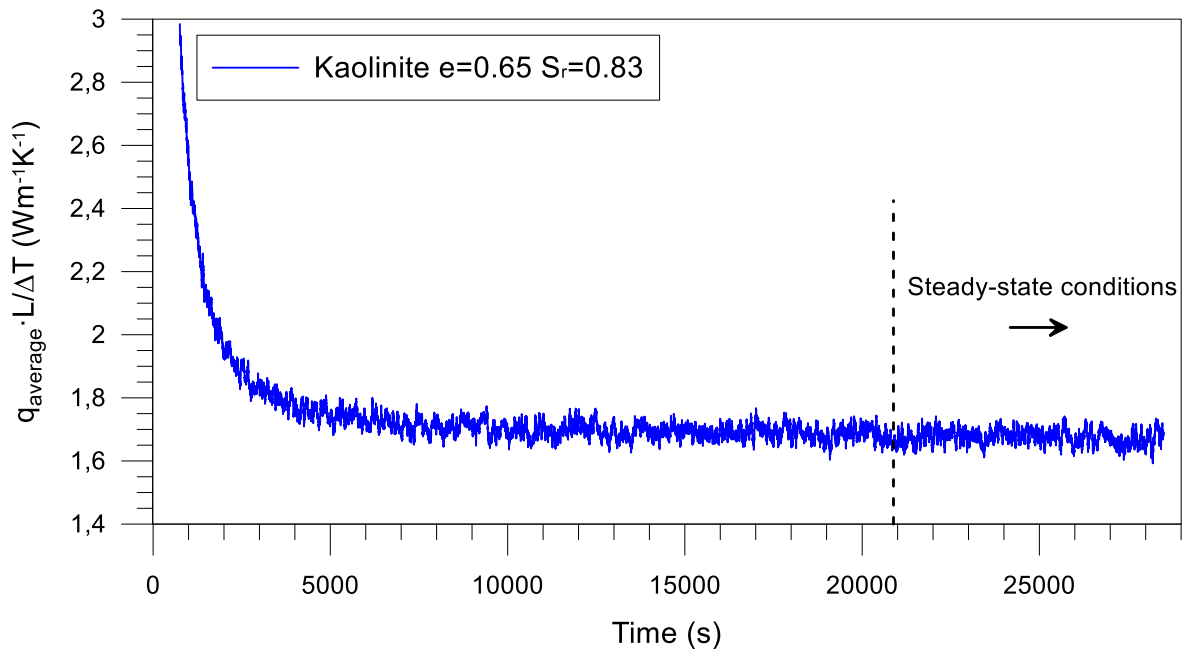


Fig. 32 Time evolution of $q_{ave} \cdot L / \Delta T$. Thermal conductivity at steady-state conditions for all tests.

- Kaolinite e=0.96Sr=0.93

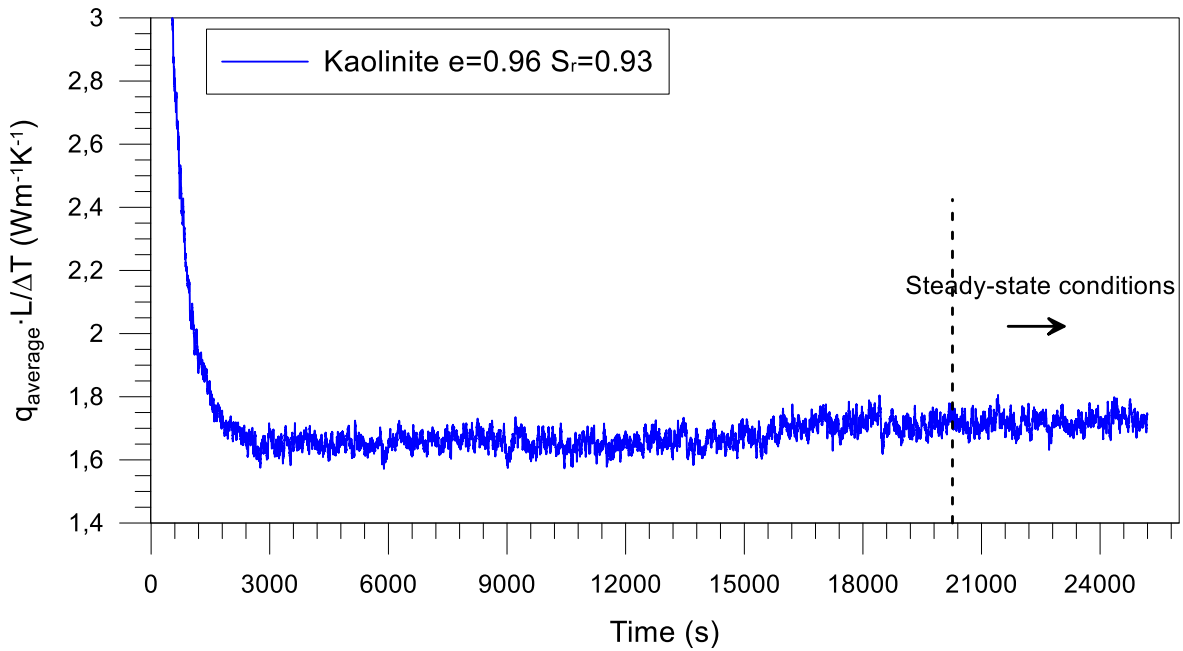


Fig. 33 Time evolution of $q_{ave} \cdot L / \Delta T$. Thermal conductivity at steady-state conditions for all tests.

- Kaolinite e=0.82Sr=0.95

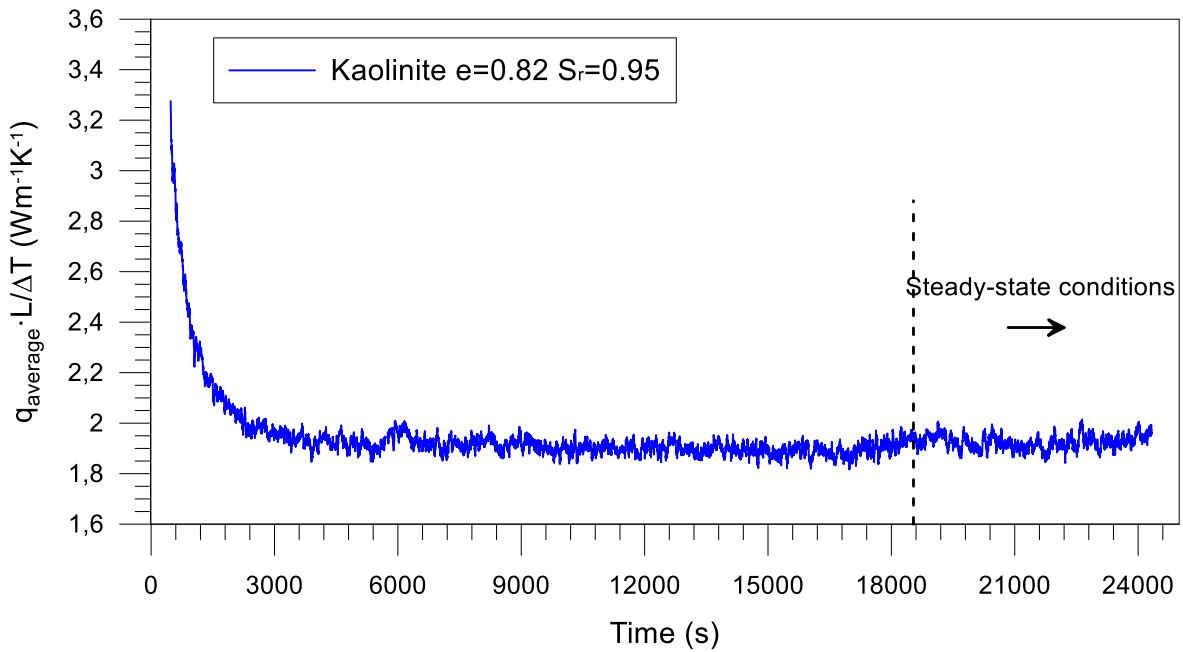


Fig. 34 Time evolution of $q_{ave} \cdot L / \Delta T$. Thermal conductivity at steady-state conditions for all tests.

▪ Kaolinite $e=0.71$ $S_r=0.93$

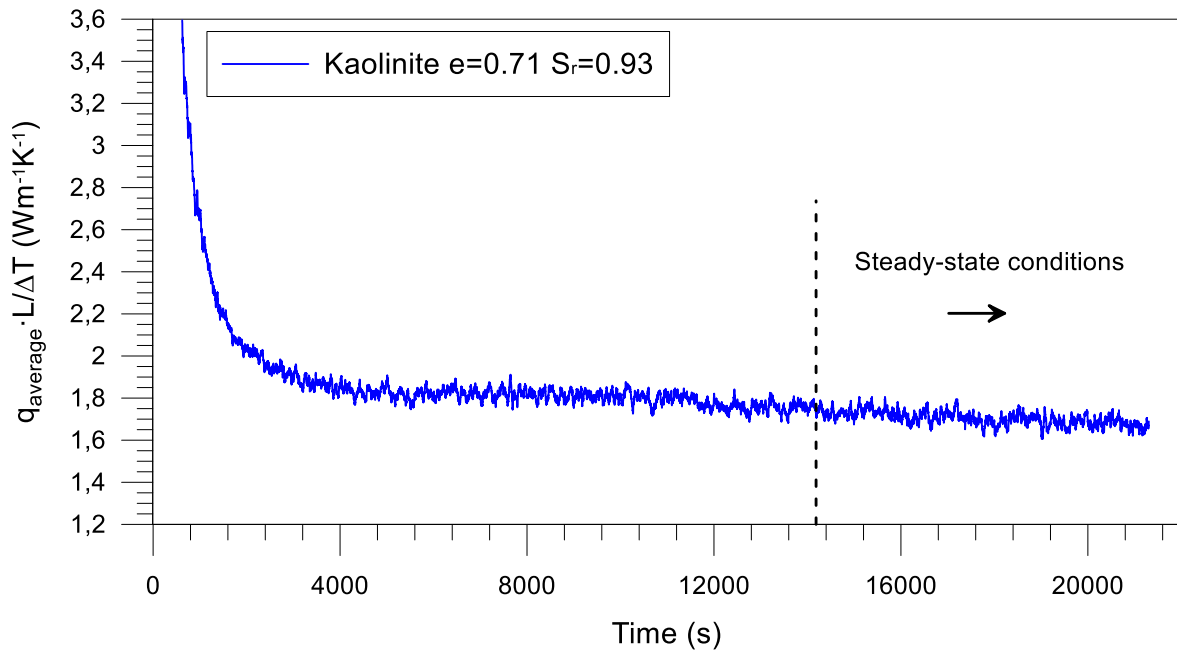


Fig. 35 Time evolution of $q_{ave} \cdot L / \Delta T$. Thermal conductivity at steady-state conditions for all tests.

▪ Illite $e=0.59$ $S_r=0.93$

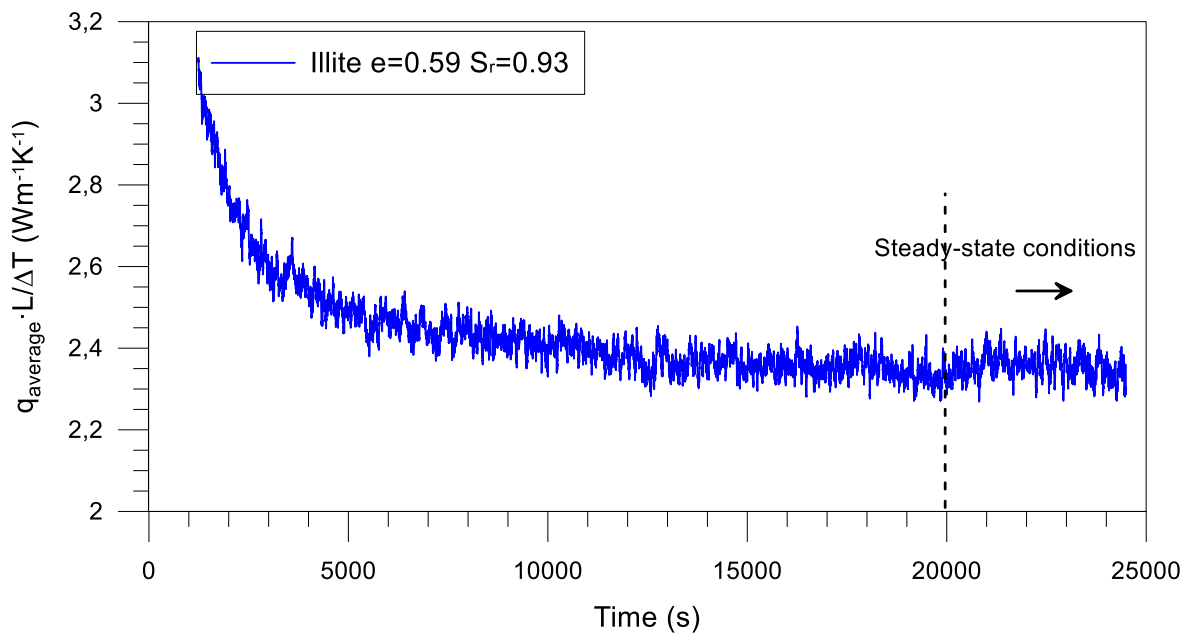


Fig. 36 Time evolution of $q_{ave} \cdot L / \Delta T$. Thermal conductivity at steady-state conditions for all tests.

- Illite e=0.72 Sr=0.81

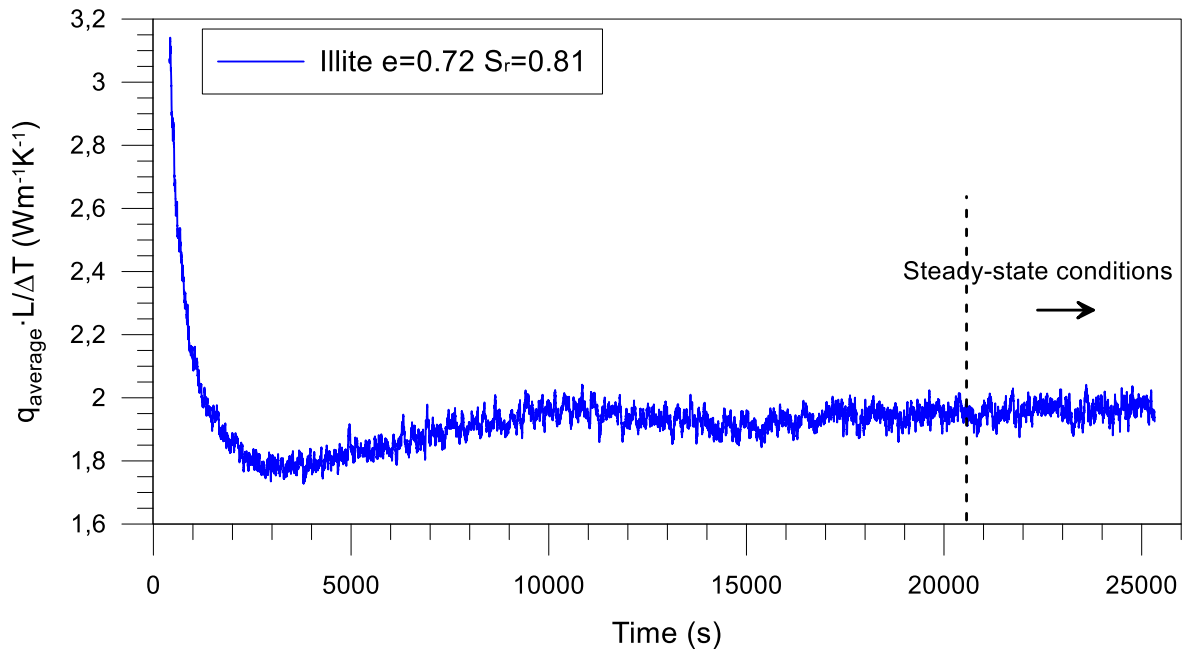


Fig. 37 Time evolution of $q_{ave} \cdot L / \Delta T$. Thermal conductivity at steady-state conditions for all tests.

- Illite e=0.72 Sr=0.67

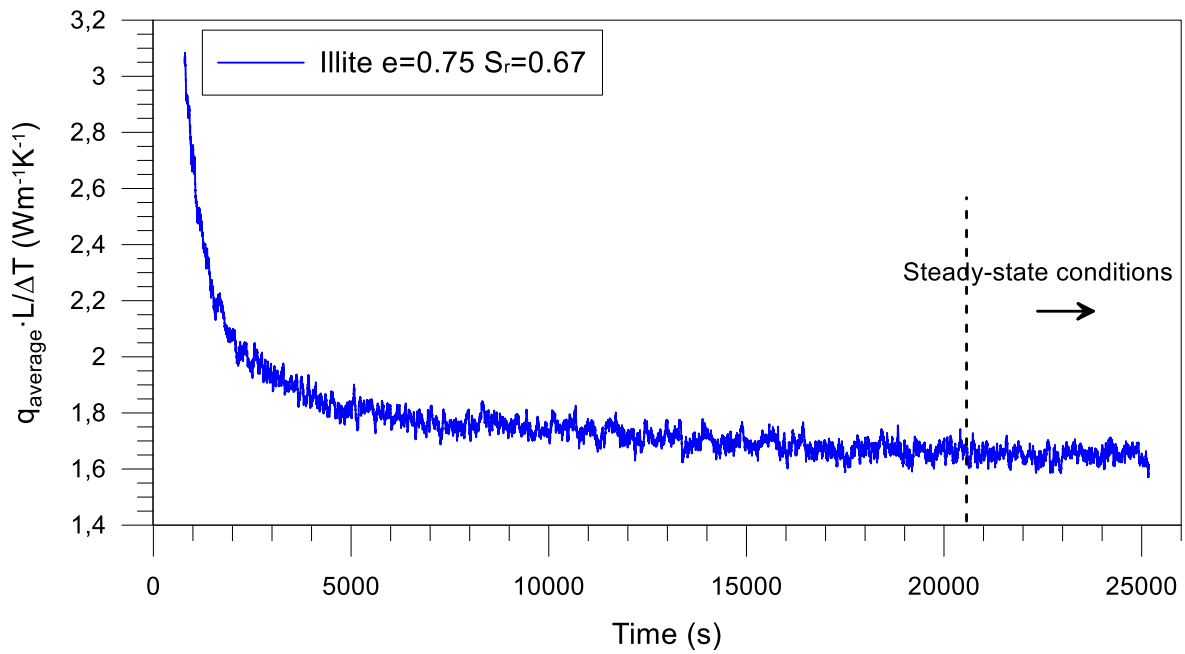


Fig. 38 Time evolution of $q_{ave} \cdot L / \Delta T$. Thermal conductivity at steady-state conditions for all tests.

▪ Illite e=0.72 Sr=0.93

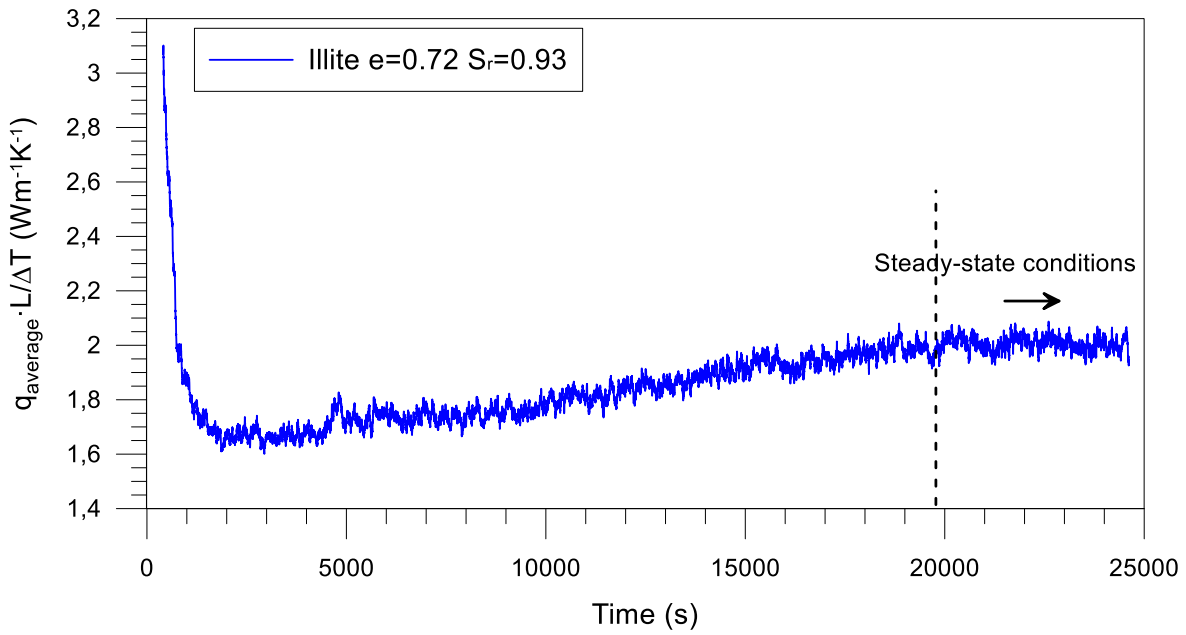


Fig. 39 Time evolution of $q_{ave} \cdot L / \Delta T$. Thermal conductivity at steady-state conditions for all tests.

▪ Illite e=0.86 Sr=0.92

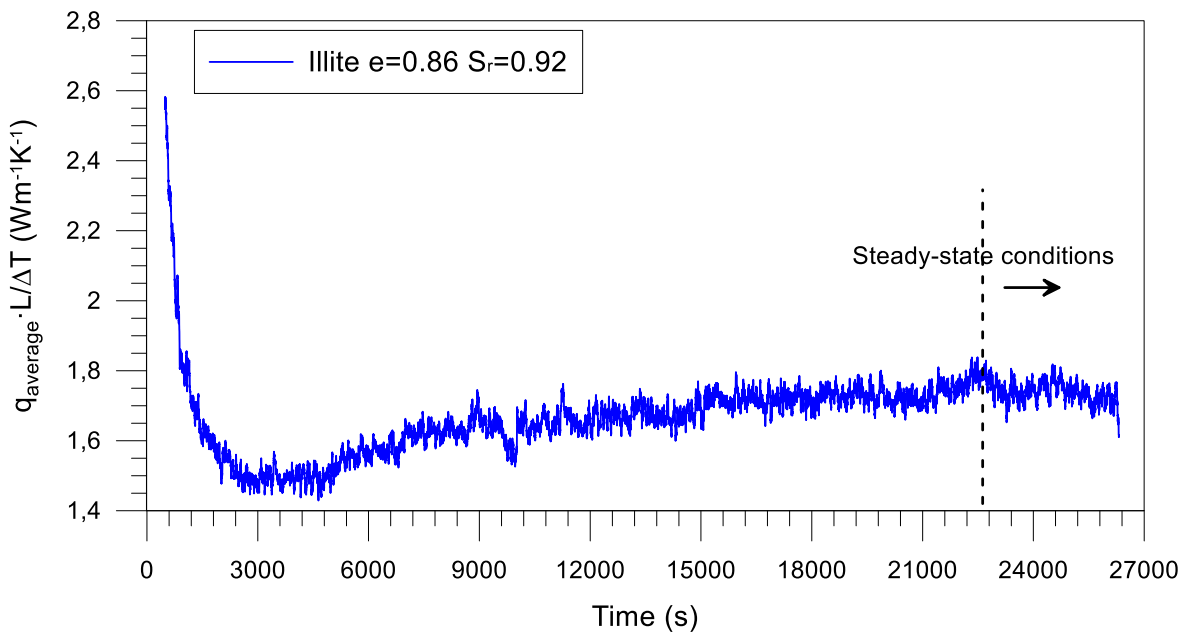


Fig. 40 Time evolution of $q_{ave} \cdot L / \Delta T$. Thermal conductivity at steady-state conditions for all tests.

Appendix C: Summary of thermal parameters

Table.1. Specific heat values obtained through tests and empirical model.

SPECIFIC HEAT				
Sample	Void ratio, e (-)	Degree of saturation, Sr (-)	Model, c (J/Kg·C)	Test, c (J/Kg·C)
ON-Kallo1-022a-mod	0.71	0.88	1597.35	1284
ON-Kallo1-022a-mod	0.71	0.73	1551.37	1169
ON-Kallo1-022a-mod	0.85	1.00	1800.60	1592
ON-Kallo1-022a-mod	0.71	1.00	1701.94	1501
ON-Kallo1-103a-mod	0.88	1.00	1684.63	1596
ON-Kallo1-103a-mod	0.71	0.71	1530.56	1357
ON-Kallo1-103a-mod	0.88	1.00	1757.88	1646
ON-Kallo1-103a-mod	0.60	1.00	1610.87	1371
Illite	0.75	0.83	1592.73	1429
Illite	0.61	0.98	1598.27	1421
Kaolinite	0.80	0.95	1805.62	1649
Kaolinite	0.72	0.93	1723.21	1515
Mix-ON-Kallo1-022a-mod-Qz-10%	0.75	0.99	2170.14	1552
Mix-ON-Kallo1-022a-mod-Qz-20%	0.74	0.99	2125.26	1590

Thermal properties in artificially prepared samples mimicking deep Ypresian clays
Appendices

Table.2 Experimental values of thermal conductivity

Sample	Void ratio, e (-)	Degree of saturation, Sr (-)	Thermal conductivity λ (W/m*K)
ON-Kallo1-022a-mod	0.85	1.00	1.88
ON-Kallo1-022a-mod	0.71	1.00	2.10
ON-Kallo1-022a-mod	0.58	0.98	2.03
ON-Kallo1-022a-mod	0.74	0.85	1.80
ON-Kallo1-022a-mod	0.68	0.75	1.86
ON-Kallo1-103a-mod	0.72	1.00	1.84
ON-Kallo1-103a-mod	0.69	0.86	1.72
ON-Kallo1-103a-mod	0.70	0.70	1.68
ON-Kallo1-103a-mod	0.59	1.00	1.91
ON-Kallo1-103a-mod	0.86	1.00	1.68
Kaolinite	0.82	0.95	2.60
Kaolinite	0.81	0.80	2.40
Kaolinite	0.83	0.65	1.96
Kaolinite	0.96	0.93	2.02
Kaolinite	0.71	0.93	2.74
Illita	0.59	0.93	2.34
Illita	0.72	0.93	2.01
Illita	0.86	0.92	1.74
Illita	0.72	0.81	1.96
Illita	0.75	0.67	1.66
Mix-ON-Kallo1-022a-mod-Qz-21%	0.74	0.98	2.21
Mix-ON-Kallo1-022a-mod-Qz-21%	0.71	0.84	1.92
Mix-ON-Kallo1-022a-mod-Qz-21%	0.72	0.69	1.68
Mix-ON-Kallo1-022a-mod-Qz-31%	0.75	1.00	2.53
Mix-ON-Kallo1-022a-mod-Qz-31%	0.71	0.85	2.41
Mix-ON-Kallo1-022a-mod-Qz-31%	0.73	0.71	2.24